Temporal change with rock magnetic properties of volcanic ashes ejected during a one-year eruption event: A case study on the Aso Nakadake 2019–2020 eruption

Chisato Anai (chisato@kochi-u.ac.jp)
Kochi University: Kochi Daigaku
Takahiro Ohkura
Kyoto University of Education: Kyoto Kyoiku Daigaku
Shin Yoshikawa
Kyoto University: Kyoto Daigaku
Nobutatsu Mochizuki
Kumamoto University: Kumamoto Daigaku

Research Article

Keywords: Coercivity, saturation magnetization, saturation remanent magnetization, single domain, Volcanic ash, Aso Nakadake volcano

Posted Date: July 22nd, 2022

DOI: https://doi.org/10.21203/rs.3.rs-1849539/v1

Version of Record: A version of this preprint was published at Earth, Planets and Space on February 20th, 2023. See the published version at https://doi.org/10.1186/s40623-023-01783-x.

Abstract

We investigated temporal changes in the magnetic properties of volcanic ash ejected from the Aso Nakadake volcano during a sequence of ash eruptions from 2019 to 2020. Titanium-rich titanomagnetite and titanium-poor titanomagnetite were the dominant magnetic minerals in the samples where titanium-rich titanomagnetite was more dominant. From the rock magnetic measurements, parameters such as the saturation remanent magnetization (M_{rs}), saturation magnetization (M_s), coercivity (B_c), and titanium content estimated from the Curie temperature (Tc) were extracted and checked for their temporal changes. The magnetic behavior of the magnetic minerals was confirmed by the increasing values of M_{rs}/M_s and B_c at several periods. The samples with higher values of M_{rs}/M_s and B_c included titanomagnetite with a low Tc (high titanium content). The clear increase in M_{rs}/M_s and B_c suggests that the ratio of the single-domain volume fraction increased, indicating that the titanomagnetite particles became finer in size. Interestingly, the periods of high M_{rs}/M_s and B_c were synchronized with observations of the volcanic glow. These results suggest that changes in the magnetic properties of volcanic ash reflect changes in physical and/or thermal conditions from the vent to the conduit.

Introduction

The magnetic minerals in the volcanic ash are dominated by titanomagnetite. Notably, the composition of titanomagnetite reflects oxygen fugacity and temperature during crystallization (Buddington and Lindsley 1964). Therefore, the magnetic properties of titanomagnetite can reflect its eruption process. However, these are simulated during relatively slow cooling, and ejecta from continuous eruptions do not necessarily exhibit the same behavior. Bowles et al. (2013) and Jackson and Bowles (2014) reported that titanomagnetite retained at around 300˚C changes in a composition called “ emplacement temperature.” This compositional change possibly records information about the magma surface phenomena inside the volcanic conduit. Magnetic minerals are characterized by magnetic properties that vary with the particle size and shape (Dunlop, 2002b). In particular, size is an important factor; finer magnetic minerals (single-domain size) tend to have a ratio of saturation remanent magnetization to remanent magnetization (M_{rs}/M_s) close to 0.5, and the coercivity (B_c) value increases. The grain-size distribution of magnetic minerals can be estimated by obtaining the parameters of the hysteresis loop. The hysteresis data of volcanic ash from ash eruptions can be systematically obtained to determine the time variation of the grain size of magnetic minerals.

In this study, we collected volcanic ash ejected from a 1-year intermittent magmatic ash eruption from July 2019 to June 2020 at the Aso Nakadake Volcano. Volcanic ash was continuously collected during the time series of the ash eruptions. We performed detailed measurements on these samples to investigate temporal changes in the rock magnetic properties of volcanic ash and their possible relationship to the eruption processes.

2019–2020 Eruption And Samples

For the first crater of the Nakadake volcano in Aso, magmatic activity started on July 26, 2019, and continued until June 2020, with several pauses. An increase in volcanic gases and volcanic glow was observed during the active period, in addition to a large amount of ash fall (Miyabuchi et al., 2021, JMA, 2021). These series of eruptions differed from the typical eruptive cycle (after the decrease of the crater lake, phreatic eruptions, ash eruptions, and Strombolian eruptions occur, and the crater lake is formed again) of the Nakadake Volcano (Yoshikawa and Sudo, 2004; Sudo et al., 2006), as it consisted of ash eruptions only.

Volcanic ash was collected from eight sites that were included in the observation points of the Aso Volcanological Laboratory, Kyoto University. This study focused on the volcanic ashes at four sampling sites, Kako-fuchi (KAF), Hondo observatory (HOND), Sakanashi (SAK), and National Aso Youth Friendship Center (AYFC), whose distances and directions from the first crater of the Nakadake volcano are approximately 250 m WSW, 1000 m SW, 7000 m NE, and 4400 m NNE, respectively. At the KAF and HOND sites, we collected volcanic ash that had fallen on solar panels for volcanic observation equipment. At the SAK and AYFC sites, volcanic ash samples were collected from the ashes accumulated on the windshield of a car. The amount of ash per unit area was unconsidered at all sites. Ashes were collected approximately 24 h after the ash falls were observed, which is quasi-real-time to individual eruptions. Notably, the ash falls occurred after individual ash eruptions during the one-year eruption period.

The collected ash samples were washed with deionized water using an ultrasonic cleaner for 10 min and dried at 60°C for 2 h.

Rock Magnetic Experiment

Various rock magnetic measurements were performed on ash samples. Forty-four samples were used for the measurements: 26 samples from KAF, 12 samples from SAK, 5 samples from HOND, and 1 sample from AYFC. Hysteresis measurements were performed using a vibrating sample magnetometer (VSM; model 3900 MicroMag, Lake Shore (PMC)) at the Center for Advanced Marine Core Research, Kochi University (KCC). For all ash samples, hysteresis loops were measured with a maximum field of 1 T. The saturation magnetization (M_s), saturation remanent magnetization (M_{rs}), and coercivity (B_c) were obtained after correcting for the paramagnetic linear contribution. First-order reversal curve (FORC) measurements were also conducted for all the samples using VSM at KCC. FORC analysis provides information about the magnetic response of all particles in a sample in terms of magnetization, represented by the magnitude of the FORC distribution, and the coercivity and magnetic interaction field distributions (shown by the Bc and Bu axes of the FORC diagram, respectively), where contrasting features can be used to diagnose the full range of magnetic domain states in fine magnetic particle systems (Roberts, et al., 2018). To identify magnetic minerals, thermal demagnetization of three-axis composite isothermal remanent magnetization (IRM), based on the method of Lowrie (1990), was performed after the ash samples were packed in quartz cylindrical cups (length: ~ 20 mm, diameter: ~ 22 mm). It should be noted that the ash particles in the cup were fixed. Because the volcanic ash was not consolidated, the sample was placed halfway into the quartz cylindrical cup, and the upper space was filled with glass wool to hold the sample in place. A strong magnetic field of 1 T was applied along the axis of the cup (z-axis), a moderate field of 0.3 T was applied to the y-axis, and finally a weak field of 0.1 T was applied to the x-axis. Progressive thermal demagnetization was performed to check the change in the magnetization of each component after the treatments. This method can estimate magnetic minerals using the coercivity range and unblocking temperature. Strong-field thermomagnetic analysis was used to confirm the behavior of magnetic minerals in response to heat and to determine the Curie Temperature (Tc). For thermomagnetic analyses, we used a thermomagnetic balance (NMB-2000M: Natsuhara Giken) at the Paleomagnetic Laboratory of Kumamoto University. The measurement conditions were as follows: The maximum temperature was 600°C and the hold time was 60 s. The heating/cooling rate was set to 10°C/min and the applied field was 300 mT. Heating/cooling cycles were performed in the atmosphere. The Tc was determined using the differential method described by Tauxe (1998). In this method, the Tc is estimated as follows: first, we calculate the derivative (dJ/dT) of the thermomagnetic curve, and then these data are differentiated to produce d^2J/dT^2. The maximum in the second derivative occurs at the point of maximum curvature in the thermomagnetic curve and is a reasonable estimate of the Tc.

Results Of Rock Magnetic Experiment

Thermal demagnetization of the three-axis composite IRM and thermomagnetic analysis indicated that the magnetic minerals contained in the ash samples were predominantly titanomagnetite including both, Ti-rich and Ti-poor titanomagnetite. The Ti content of Ti-rich titanomagnetite varies depending on the time of collection; however, a Tc of approximately 300°C was generally observed throughout the entire period, indicating that Ti-rich titanomagnetite of this composition is the main magnetic mineral.

The hysteresis parameters M_{rs}/M_s and B_c were determined from hysteresis loop measurements, where M_{rs}/M_s is the ratio of saturation remanent magnetization to saturation magnetization and B_c is the coercive force. These values showed a good correlation (Fig. 1c), and each changed with the time of sample collection. Generally, the larger the values of M_{rs}/M_s and B_c, the higher the single-domain (SD) volume fractions; meaning that the size distribution of magnetic grains becomes finer (Dunlop, 2002). The M_{rs}/M_s values in Fig. 1c indicate that the volcanic ash, which erupted in 2019–2020, contained magnetic minerals with particle sizes varying from multi-domain (MD) grain to SD grain sizes. Figure 2 shows a FORC diagram of some of the volcanic ash samples collected between September 2019 and January 2020 in chronological order. The results for October 14 and November 6, 2019, show the predominance of stable SD grains with high coercivity compared to those of the other periods. More detailed coercivity changes can be observed in the result of the thermal demagnetization of the three-axis composite IRM (Fig. 3). Measurements on the sample from September 14, 2019, showed a predominance of low-coercivity components below 100 mT, and a minor component above 300 mT could be identified. In contrast, the sample from October 14, 2019, showed a predominance of moderate coercivity components in the 100–300 mT range, and components with coercivity > 300 mT were confirmed. These variations were also observed in samples from January to February 2020. In addition, this behavior of B_c can be observed for both Ti-rich and Ti-poor titanomagnetite.

The results of the thermomagnetic analysis are shown in Fig. 4. Titanomagnetite ($Fe_{3-x}Ti_xO_4$) with a Tc of 300°C has a composition of approximately x = 0.4 based on the formula of Hunt et al. (1995). Depending on the timing of the eruption, some of these compositions appeared simultaneously with lower or higher Tc values. Titanomagnetite with titanium-rich compositions and Tc < 200°C (x approximately equal to 0.6) can be seen from mid-October to early November 2019, late December 2019, and late January to late February 2020. Ti-poor titanomagnetite showed a Tc phase of approximately 500°C, which was identified in a sample taken just before the cessation of the eruption in June 2020. Moreover, this sample does not contain any Tc of approximately 300°C and is systematically included in the other samples; the magnetic minerals of this sample are completely different from those of the other samples.

Temporal Changes Of Rock Magnetic Properties

We discuss how chronologically ordered changes in rock magnetic properties are related to eruptive activity. The remarkable behavior of the magnetic properties of volcanic ash was confirmed as follows: Hysteresis loop parameters of M_{rs}/M_s and B_c that show particularly significant variation increased during the periods from mid-October to early November 2019, late January to mid-February, and early June 2020. Hc is the coercivity of magnetic minerals, and its increase indicates that the stability of the magnetic minerals is enhanced. As M_{rs}/M_s and B_c increase, the magnetic mineral becomes closer to the SD grain, which is a more stable magnetic property.

The periods of high values in M_{rs}/M_s and B_c were mid-October to early November 2019, late January to mid-February, and early June 2020. The values of M_{rs}/M_s and B_c were larger during this period, indicating that the contribution of the SD particles increased significantly. The temporal change in the FORC diagram (Fig. 2) shows an increase in coercivity and the contribution of non-interacting SD grains from September to October 2019, which is consistent with the behavior of M_{rs}/M_s and B_c. The predominance of the 100–300 mT component in the IRM-TD measurement also coincided with the period when the component above 300 mT could be confirmed (Fig. 3). The increase in the SD volume fraction was probably due to the increased supply of SD titanomagnetite. However, the value of Ms per unit weight did not correlate with the variation indicated by the M_{rs}/M_s and B_c parameters. Because the value of M_s per unit weight is a parameter indicating the total amount of magnetic minerals, it can be considered that the total amount of magnetic minerals did not change but the MD-like magnetic minerals changed to SD grains with changes in temporal volcanic activity. The results of the September 4, 2019, FORC diagram show the typical MD grain character (Roberts et al., 2018), where the distribution of Bu values on the low-coercivity side is broadened. This feature is common to periods when magnetic minerals with low coercivity dominate. Because MD grains are known to have a larger grain size and lower coercivity than SD grains, it is estimated that the volume fraction of MD grains is high during periods when low coercivity magnetic materials predominate. Particularly, during a series of eruption activities, magnetic particles in volcanic ash, which are composed of MD + SD grains, possibly temporarily increase the volume fraction of SD grains.

The results of the rock magnetic measurements indicate that magnetic minerals in volcanic ash have periods of increased SD and Ti-rich titanomagnetite grains, which have slightly lower Tc than those of the other periods (Fig. 4). This period of dominance of SD grains was named the “fine titanomagnetite period (FTP)” and its relationship to volcanic phenomena is discussed below.

Comparison With Volcanic Phenomena

The first crater of Nakadake volcano, Aso, magmatic activity started on July 26, 2019, and the eruptions continued until June 15, 2020, with multiple pauses. During the active period, a large amount of ash fall, an increase in volcanic gases, and volcanic glow events over the crater were observed (Miyabuchi et al., 2021). Contrasting various observational data with the rock magnetic results of this study suggests that the results are related to volcanic glow observations according to the Japan Meteorological Agency (JMA). Volcanic glow events were frequently observed from late July to early August 2019, early October to mid-November and late December 2019, and late January to late February 2020. The FTP coincides well with the observed volcanic glow period (JMA, 2021, Fig. 5). As mentioned in the previous section, FTP is the time when the SD particles increase and titanomagnetite with a high titanium content is identified. The conditions under which the magnetic minerals change are discussed. The value of Ms per unit weight does not correlate clearly with changes in the values of M_{rs}/M_s or B_c, and it can be considered that the variation in M_{rs}/M_s and B_c is not due to the supply of total magnetic minerals in the magma. Since MD particles have a larger particle size than SD particles, it is thought that the time required for crystal growth from crystallization to cooling is longer than that for SD particles. This implies that physical and/or thermal changes inside the conduit are altered during the eruption process, and that the magnetic minerals reflect these changes. Moreover, the coincidence of the increase in SD volume fraction and the timing of the observation of volcanic glow also support the idea that FTP is capturing the phenomena inside the conduit. Mujin and Nakamura (2014) noted changes in particle size as the magma rose; they found that when the magma head was located deep inside the crater, relatively large particles were crystallized due to depressurization and a calm temperature gradient, but as the magma head rose, finer particles were newly formed owing to the effects of degassing, rapid cooling, and oxidation. Their assertions support the results of this study, and it will be important to examine the correspondence with the results obtained from physical observations in the future. This indicates that the rock magnetic properties of volcanic ash can contribute to the elucidation of the eruption process.

Conclusion

In this study, rock magnetic analyses were conducted on volcanic ash ejected by the one-year intermittent eruptive activity of the Aso Nakadake Volcano from July 2019 to June 2020. Ti-rich and Ti-poor titanomagnetite were the main magnetic minerals in the volcanic ash, where the former was dominant. The magnetic properties of titanomagnetite vary depending on the timing of the eruption, with particularly high values of the ratio of saturation remanent magnetization to saturation magnetization (M_{rs}/M_s) and coercive force (B_c). In addition, the ash samples with high M_{rs}/M_s and B_c also show Ti-rich and Ti-poor titanomagnetite, but the Ti-rich phase has a slightly higher Ti content than the samples with low M_{rs}/M_s and B_c. The increased values of M_{rs}/M_s and B_c indicate a higher volume fraction of the SD titanomagnetite particles. The SD predominance indicates a finer titanomagnetite predominance. Our results revealed that the periods of high M_{rs}/M_s and B_c coincided with the timing of the volcanic glow events. The results of this study suggest that temporal changes in the rock magnetic properties of volcanic ash are related to temporal changes in the physical conditions of the crater during eruptive activity.

List Of Abbreviations

National Aso Youth Friendship Center (AYFC)

Fine titanomagnetite period (FTP)

First-order reversal curve (FORC)

Hondo observatory (HOND)

Isothermal remanent magnetization (IRM)

Kako-fuchi (KAF)

Kochi University (KCC)

MicroMag, Lake Shore (PMC)

Multi-domain (MD)

Sakanashi (SAK)

Single-domain (SD)

Vibrating sample magnetometer (VSM

Declarations

Ethics approval and consent to participate

Not applicable

Consent for publication

Not applicable

Availability of data and materials

Competing interests

Not applicable

Funding

This study was funded by the Earthquake Res. Institute, University of Tokyo Joint Research Program,< Accept No. 2021-KOBO23>. This study was also performed under the cooperative research program of the Center for Advanced Marine Core Research, Kochi University, <Accept No.19B064>.

Authors' contributions

Chisato Anai treated the samples, conducted all experiments, and wrote the manuscript. Takahiro Ohkura corrected all ash samples and assisted in constructing the framework of this study and the manuscript. Shin Yoshikawa assisted in correcting and treating the samples and rock magnetic experiments. Nobutatsu Mochizuki assisted with the rock magnetic experiments and drafted the manuscript.

Acknowledgements

We would like to thank Hidetoshi Shibuya, Akihiko Yokoo, and Mitsuru Ustugi for their helpful discussions on this research. We also thank Yuhji Yamamoto and Tadahiro Hatakeyama for their help in conducting the measurements at the Kochi Core Center.

References

1. Bowles JA, Jackson MJ, Berquó TS, Sølheid PA, Gee JS (2013) Inferred Time- and Temperature-Dependent Cation Ordering in Natural Titanomagnetites. Nat Commun 4(May). DOI: 10.1038/ncomms2938
2. Buddington AF, Lindsley DH (1964) Iron-Titanium Oxide Minerals and Synthetic Equivalents. J Petrol 5(2):310–357. https://doi.org/10.1093/petrology/5.2.310
3. Dunlop DJ, Özdemir Ö (1997) Rock Magnetism: Fundamentals and Frontiers (No.3). Cambridge University Press
4. Hunt CP, Moskowitz BM, Banerjee SK (1995) Magnetic properties of rocks and minerals. In: Ahrens TJ (ed) Rock Physics & Phase Relations: a handbook of physical constants. AGU Reference Shelf 3
5. Jackson M, Bowles JA (2014) Curie temperatures of titanomagnetite in ignimbrites: Effects of emplacement temperatures, cooling rates, exsolution, and cation ordering. Geochem Geophys Geosyst 15(11):4343–4368. https://doi.org/10.1002/2014GC005527

6. Japan Meteorological Agency (2021) Annual Volcanic Activity Report (2020). https://www.data.jma.go.jp/svd/vois/data/tokyo/STOCK/monthly_v-act_doc/fukuoka/2020y/503_20y.pdf
7. Lowrie W (1990) Identification of Ferromagnetic Minerals in a rock by coercivity and unblocking temperature properties. Geophys Res Let 17(2):159–162. https://doi.org/10.1029/GL017i002p00159
8. Miyabuchi Y, Iizuka Y, Futa E, Ohkura T (2021) Precursor Activity of the 2019–2020 Magmatic Eruption at Nakadake First Crater, Aso Volcano: Insights from Ash Fall Deposits from Early Activity on May 3–5, 2019. Bull Volcanol Soc Japan 66(3):157–169 (in Japanese with English abstract). https://doi.org/10.18940/kazan.66.3_157
9. Mujin M, Nakamura M (2014) A Nanolite Record of Eruption Style Transition. Geology 42(7):611–614. https://doi.org/10.1130/G3553.1
10. Roberts AP, Zhao X, Harrison RJ, Heslop D, Muxworthy AR, Rowan CJ, Larrasoaña JC, Florindo F (2018) Signatures of Reductive Magnetic Mineral Diagenesis From Unmixing of First-Order Reversal Curves. Jou Geophys Res : Solid Earth 123(6):4500–4522. https://doi.org/10.1029/2018JB015706
11. Sudo Y, Tsutsui T, Nakaboh M, Yoshikawa M, Yoshikawa S, Inoue H (2006) Ground Deformation and Magma Reservoir at Aso Volcano: Location of Deflation Source Derived from Long-Term Geodetic Surveys. Bull Volcanol Soc Jpn 51(5):291–309 (in Japanese with English abstract). https://doi.org/10.18940/kazan.51.5_291
12. Tauxe L (1998) Paleomagnetic Principles and Practice. Kluwer Academic Publishers, Dordrecht, p 299
13. Yoshikawa S, Sudo Y (2004) Volcanic Activity and Surface Temperature Varietion of Crater Lake in Naka-Dake Crater at Aso Volcano. Annuals of Disas Prev Res Inst Kyoto Univ 47(B):1–3 in Japanese with English abstract

Figures

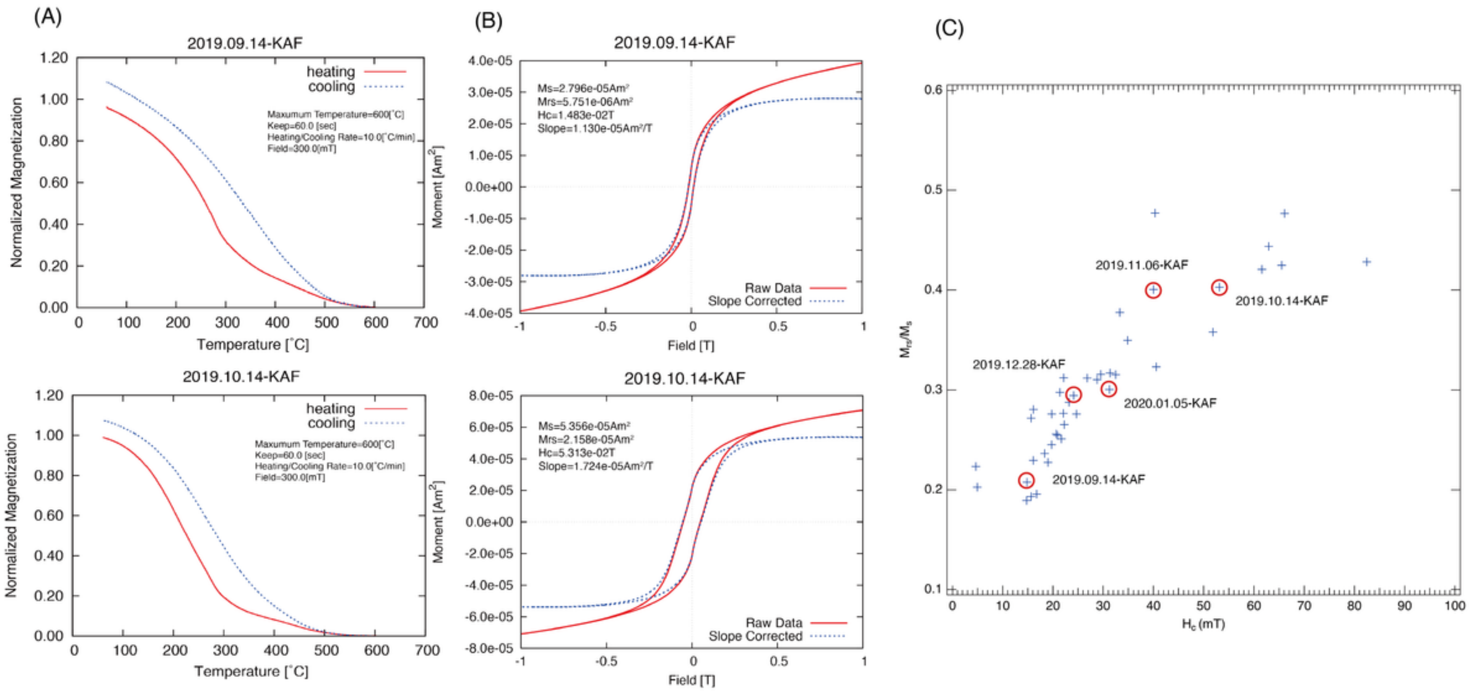

Figure 1

Results of thermomagnetic analysis and hysteresis measurements. (A) Examples of thermomagnetic analysis. The solid red line is heating curve and blue dashed line is cooling curve, respectively. (B) Examples of hysteresis measurements. The solid red line is the measured hysteresis loop (raw data). The blue dashed line is the corrected loop for the effect of paramagnetic minerals. (C) A plot of the ratio of saturation remnant magnetization to saturation magnetization (M_{rs}/M_s) vs Coercivity (B_c). The upper right of the plot is the higher SD grain size, and the lower left is closer to the MD grain size. The higher M_{rs}/M_s and B_c are, the higher the volume ratio of a single domain (SD) grains to multidomain (MD) grains.

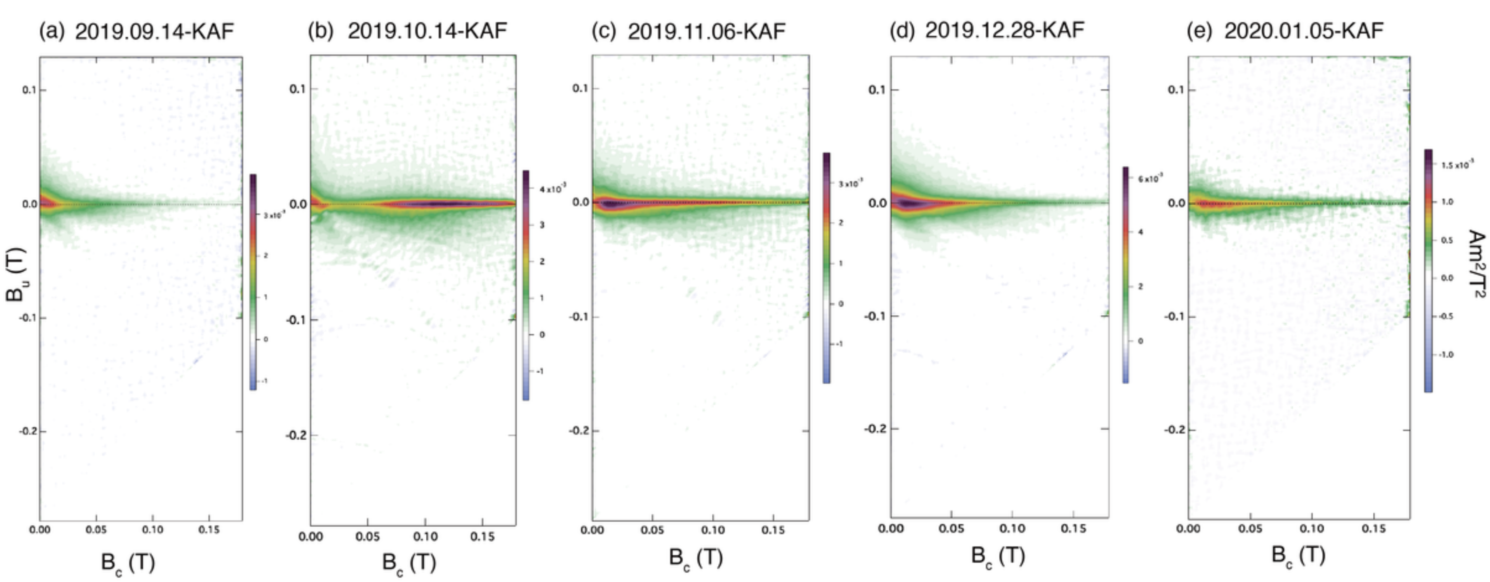

Figure 2

FORC diagram in chronological order. All data for samples collected from the KAF station; ash samples of October 14 and November 6, 2019 (b and d), the presence of stable SD particles with high coercivity, and a narrow range of Bu values.

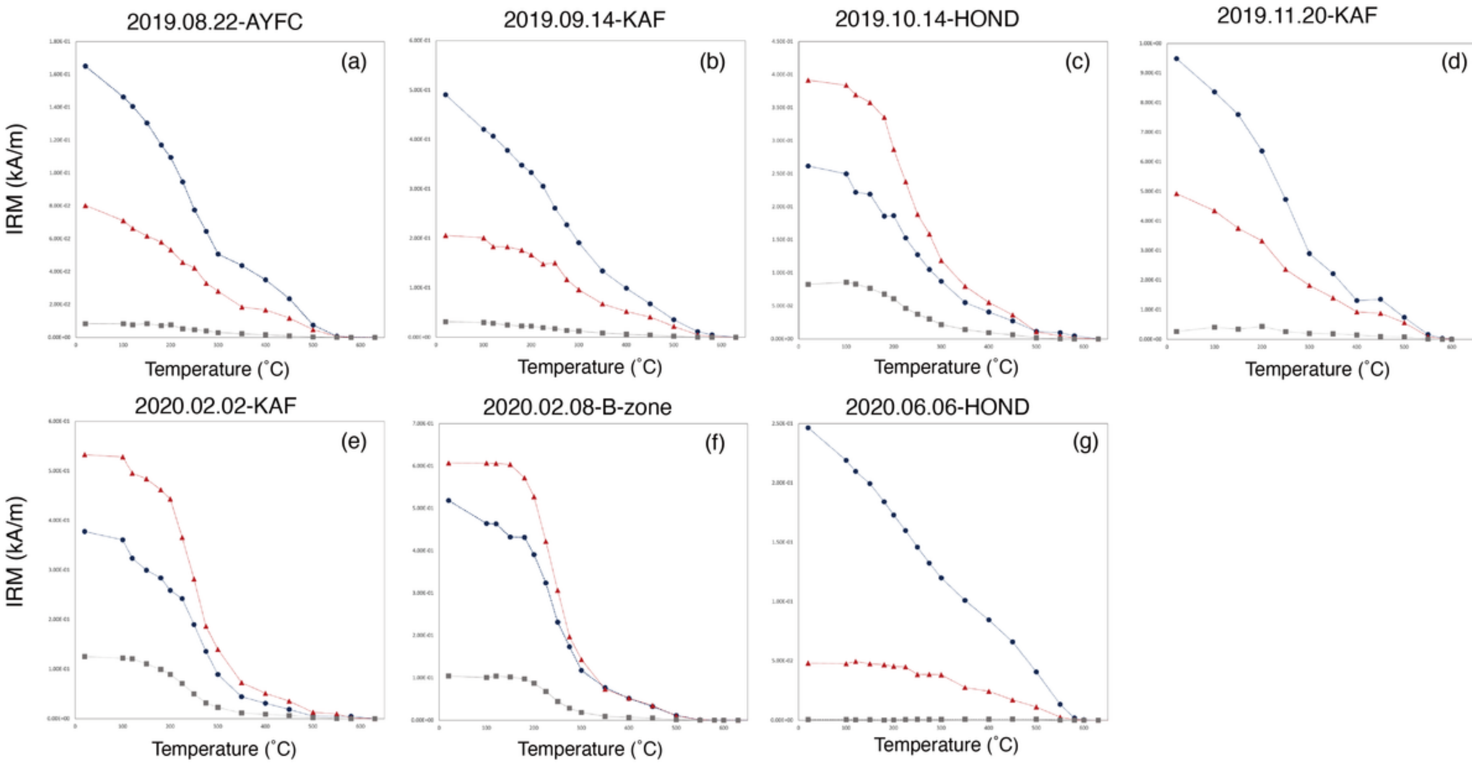

Figure 3

Thermal demagnetization of 3-axis composite IRM. IRM components of coercivity ≤ 0.1 T, 0.1–0.3 T, and 0.3–1 T are shown by circles, triangles, and squares, respectively. The unblocking temperature indicates it is a mixture of titanomagnetite with different coercivity. High coercivity IRM component of 0.3–1 T can be seen during periods of predominance of the IRM component of 0.1–0.3 T (e.g., on October 14, 2019, and February 2, 2020).

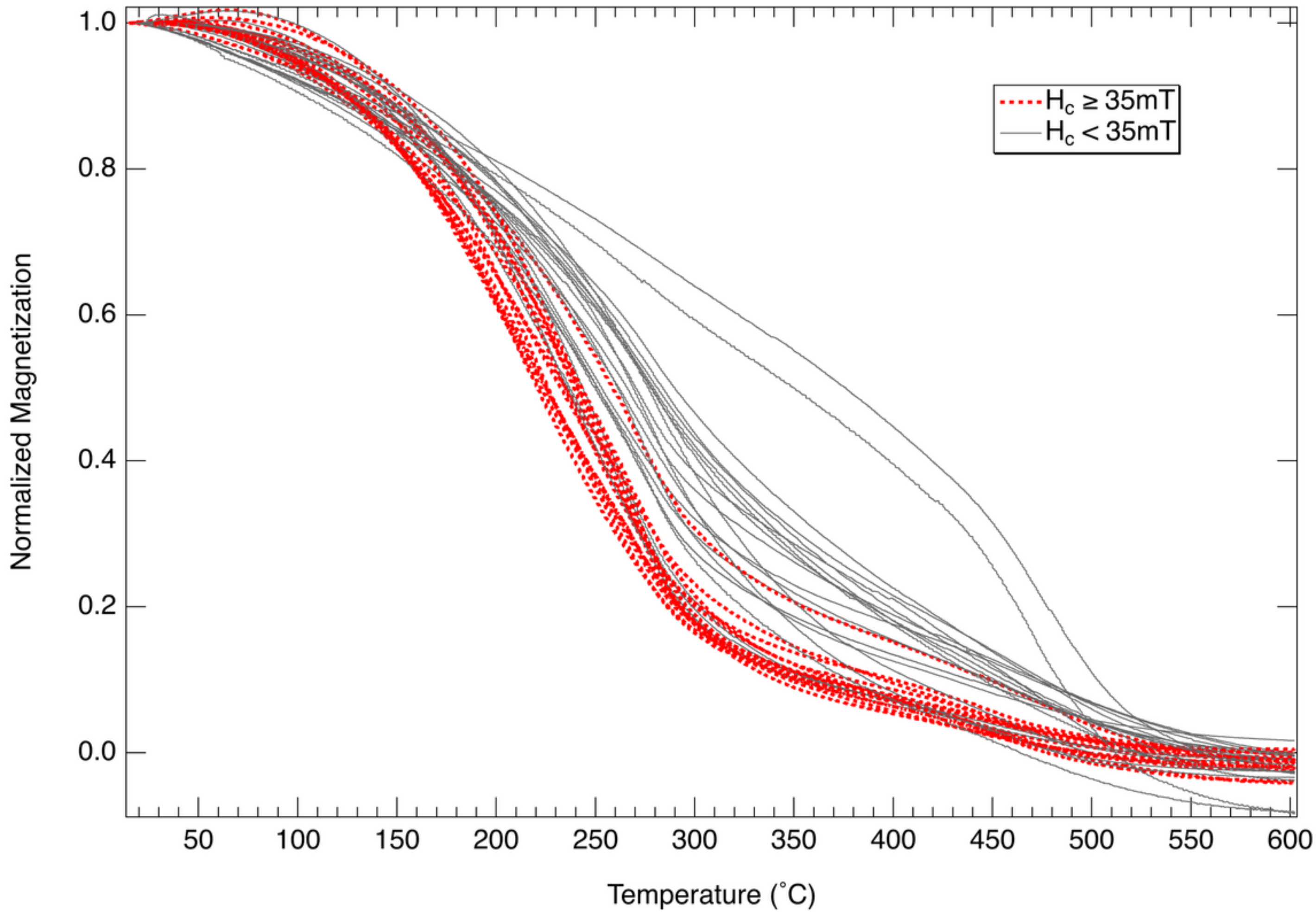

Figure 4

Results of strong field thermomagnetic analyses (heating curve) of all samples. The red dashed lines show the samples of high coercivity ($\geq$ 35 mT), and the gray lines show the samples of low coercivity (< 35 mT), respectively.

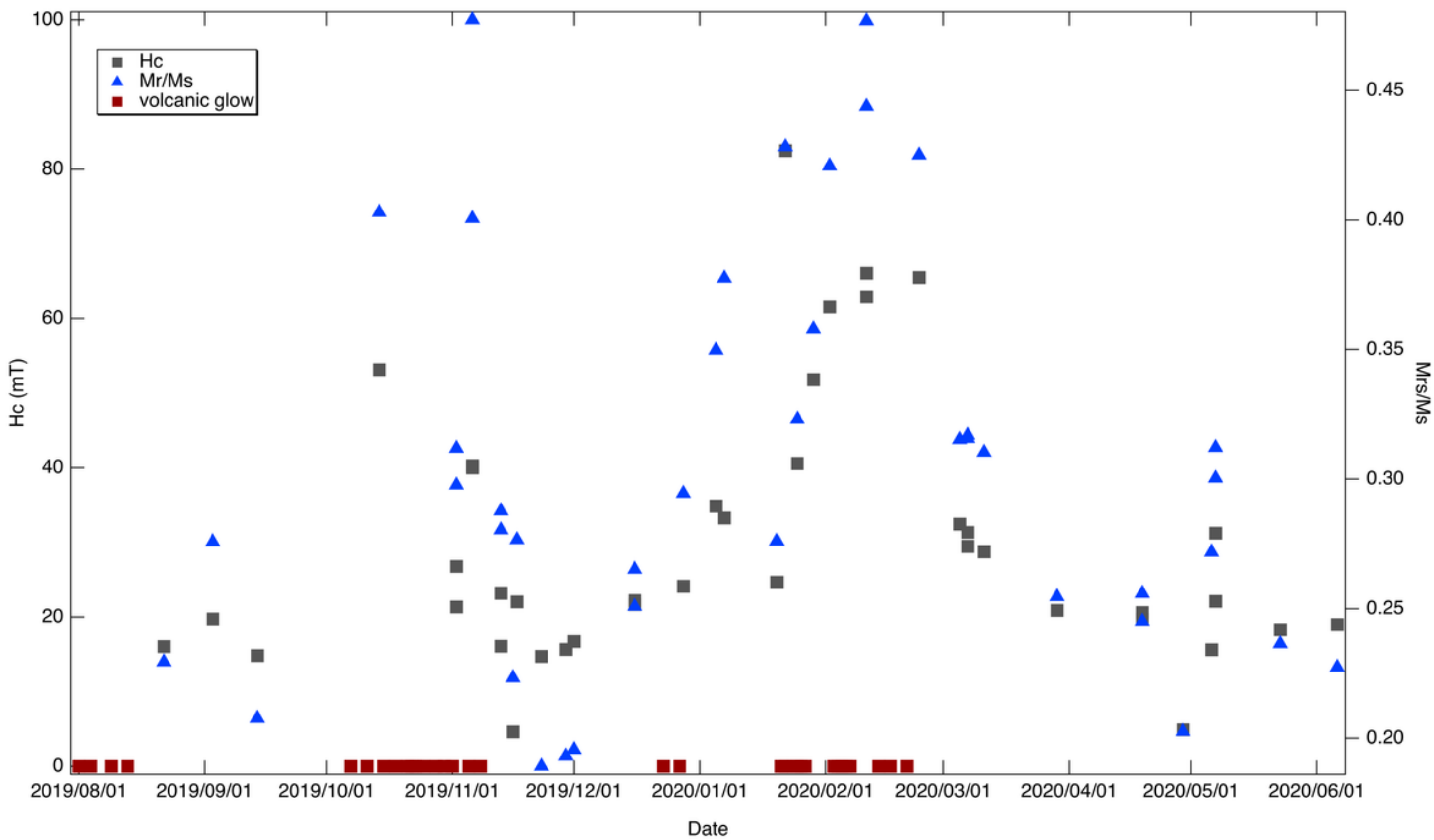

Figure 5

Hysteresis parameters (M_{rs}/M_s and B_c) in chronological order. Gray squares indicate B_c and blue triangles denote M_{rs}/M_s. Red squares indicate the day when the volcanic glow was observed. High M_{rs}/M_s and B_c mean the predominance of single domain (SD) particles.

Supplementary Files

This is a list of supplementary files associated with this preprint. Click to download.

- abstract.png